Geophys. J. Int. (1994) **116**, 553–561

Determination of seismogenic interplate contact zone and crustal seismicity around Antofagasta, northern Chile using local data

D. Comte,[1,3] M. Pardo,[1,3] L. Dorbath,[2,4] C. Dorbath,[2,4] H. Haessler,[2] L. Rivera,[2] A. Cisternas[2] and L. Ponce[3]

[1]*Depto de Geología y Geofísica, U. de Chile, Casilla* 2777, *Santiago, Chile*
[2]*Institut de Physique du Globe de Strasbourg,* 5 *Rue Rene Descartes,* 67084 *Strasbourg, Cedex France*
[3]*UACPyP, Instituto de Geofísica, UNAM, México D.F.* 04510, *México*
[4]*ORSTOM,* 213 *Rue La Fayette,* 75480 *Paris Cedex* 10, *France*

Accepted 1993 July 20. Received 1993 July 20, in original form 1992

SUMMARY

During September and October 1988 a microseismic field experiment was carried out around the city of Antofagasta, northern Chile, with 29 portable analogue and digital stations. A total of 197 reliable microearthquake locations and 19 focal mechanisms were determined. It is proposed that it is possible to estimate the maximum depth of the coupled–uncoupled transition of the subducting lithosphere using local data, defined by the depth of the expected change of the stress field from compressional to tensional along the slab. This change is observed at about 70 km depth in the Antofagasta field work. Two estimations of the width of the seismogenic interplate contact are discussed: (1) the maximum depth of the coupled zone defined by the observed maximum depth of the shallow-dipping thrust events recorded during the experiment of 47 km, corresponding to a width of the seismogenic contact zone of about 90 km; and (2) the maximum depth of the coupled zone defined by the depth of the observed change from a compressional to tensional stress field, which is 70 km and corresponds to a width of the seismogenic contact zone of about 130 km. With both values, the maximum magnitude M_S estimated for the region varies between 8.6 and 8.7. No shallow event associated with the Atacama fault system was observed during the experiment.

Key words: Atacama fault, microseismicity, northern Chile, seismogenic interplate contact, subduction morphology.

INTRODUCTION

Northern Chile has been recognized as an important seismic gap where a major earthquake is expected in the near future (Kelleher 1972; McCann *et al.* 1979; Nishenko 1985; Comte & Pardo 1991). However, the Wadati–Benioff zone is poorly established because almost all the seismic studies related to northern Chile (e.g. Barazangi & Isacks 1976; Araujo 1985; Chowdhury & Whiteman 1987; Isacks 1988) have used teleseismic data due to the lack of regional and local networks.

The area studied here is close to the southern edge of the region which ruptured during the last great ($M_w = 8.8$) 1877 earthquake (Dorbath *et al.* 1990; Comte & Pardo 1991). No major thrust event ($M_S > 7.5$) has affected the region this century. Moreover, no historical great earthquake is known to have occurred in the coastal zone south of Antofagasta (24–25°S).

During September and October 1988 a joint experiment by the University of Chile, the Institut de Physique du Globe de Strasbourg and the Institut Français de Recherche Scientifique pour le Développement en Coopération (ORSTOM) was conducted over an area of about 150 km in width around Antofagasta (northern Chile) to study the morphology of the subducted slab and the extent of the coupled zone between the Nazca and South American plates.

The extent of seismically coupled zones in subduction regions has mainly been studied using globally recorded data. Tichelaar & Ruff (1991) studied seismic coupling along the Chilean subduction zone using $M > 6$ events. However, due to the lack of significant thrust events in northern Chile since the great 1877 earthquake, reliable estimation of the maximum depth of coupling in this region using teleseismic data is uncertain.

In this study, we analysed the subduction morphology

around Antofagasta using reliable local data. We propose that it is possible to map the coupled–uncoupled transition along the subducting slab to estimate the maximum depth of the seismogenic contact zone.

Another objective of the 1988 campaign was to investigate crustal seismicity in relation to the main tectonic features. In northern Chile two mega-fault systems are present: the Atacama fault and the Coastal Scarp. The nature and kinematics of both structures are controversial: Arabasz (1971) stated that the Atacama fault acts mainly as a normal fault, whereas Armijo & Thiele (1990) observed mostly left-lateral movement along the central part. Naranjo (1987) suggests that the Atacama fault is presently inactive as a strike–slip fault, and Yañez (in preparation) indicates that the Atacama fault was very active during the Mesozoic, but may have remained inactive since the Tertiary because of the migration of the volcanic front 200 km landward.

DATA ACQUISITION AND PROCESSING

Seismological network

A seismological network of 29 portable stations was installed within a 150 km radius around Antofagasta during September–October 1988 (Fig. 1). The location of each station was determined using topographic maps (1 : 50 000) and the satellite positioning system TRANSIT. The error in the locations is estimated to be less than 150 m (Table 1).

Three types of seismic stations were used. (1) 13 MEQ-800 smoked-paper recording stations with vertical L-4C (1 Hz) seismometers. The gains were set at 84 dB with open filters and the paper speed was 60 mm min^{-1}. The drifts of the internal clocks were measured by comparing the internal time with the reference time pulses transmitted by the WWN (Colorado, USA) or LOL (Argentina) stations. (2) Eight digital GEOSTRAS variable gain stations with

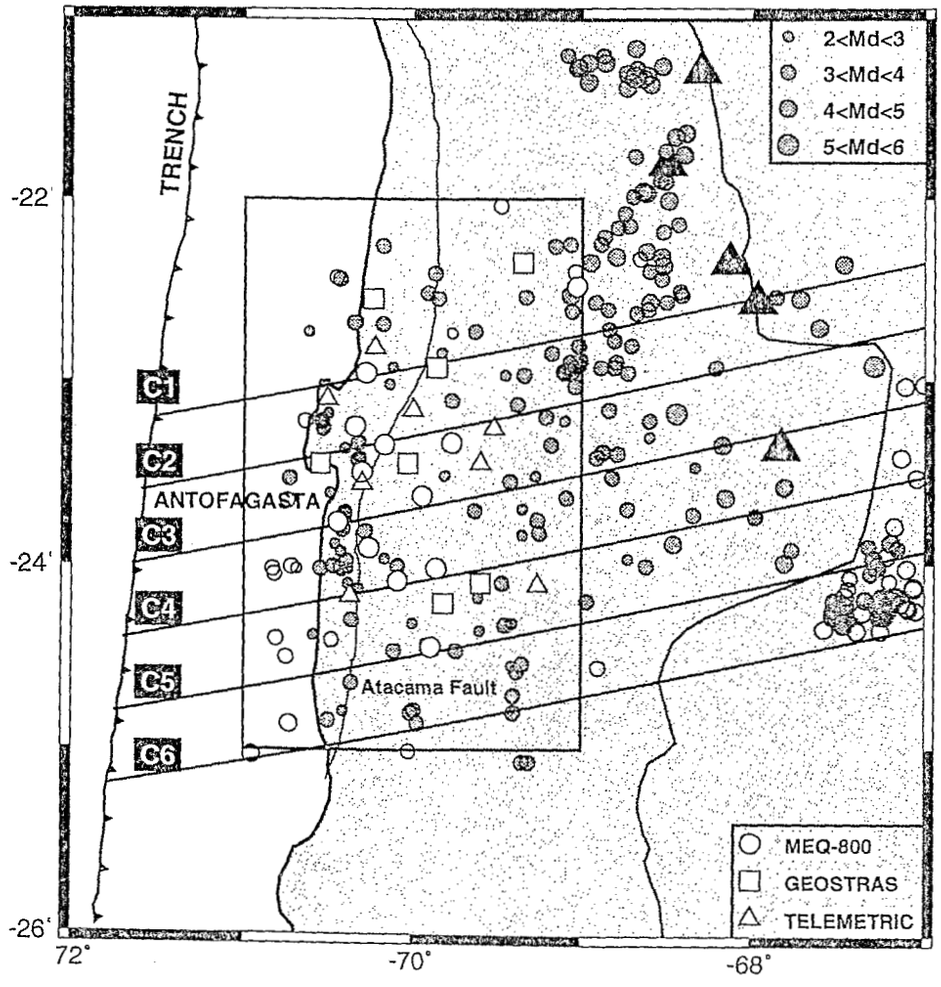

Figure 1. Distribution of the Antofagasta 1988 temporary seismic network (open symbols inland). Epicentral distribution of the seismicity recorded in this experiment. Closed circles correspond to reliable solutions and open circles denote the relocated events. The rectangle indicates the coverage of the seismic network. Six profiles in the direction of convergence are also shown. Closed triangles indicate the active volcanoes in the Andean range.

Table 1. Locations of analogue MEQ-800, digital Geostras and digital telemetric stations. Latitude and longitude are given in degrees and minutes. Elevation is in metres relative to the mean sea-level. STA is the name of the station.

STA	LAT °(S)	LON°(W)	ELEV	LOCATION
ANALOG MEQ-800 STATION				
CAL	22 28.81	69 01.52	2030	Calama
HOS	22 57.47	70 16.69	270	Hornitos
DVM	23 15.05	70 20.61	360	Desv. Mejillones
CLB	23 20.37	69 46.09	1320	Culebron
MIR	23 21.44	70 10.60	1225	Miranda
CHO	23 03.33	69 35.59	1570	Chacabuco
FAR	23 29.87	70 17.92	950	Farol
CUE	23 37.68	69 56.31	960	Cuevitas
COL	23 46.60	70 26.33	150	Coloso
TOS	23 54.86	70 15.51	720	Tosca
YUG	24 01.23	69 51.77	1250	Yugoslavia
YNG	24 05.36	70 05.14	1070	Yungay
ROS	24 27.43	69 53.50	1470	Rosario
DIGITAL GEOSTRAS STATION				
SRA	22 51.98	69 20.84	1800	Sierra Gorda
TAM	22 38.71	70 14.58	270	Tamira
ESM	22 56.04	69 51.99	1510	Esmeralda
MBL	23 27.27	70 01.62	840	Mantos Blancos
MOR	23 30.58	70 33.02	220	Moreno
MAG	24 05.72	69 35.80	1400	Magnesia
SGR	24 13.06	69 49.50	1130	San Gregorio
LVI	24 28.99	70 18.89	1930	Los Vientos
DIGITAL TELEMETRIC STATION				
LVI	24 28.99	70 18.89	1930	Los Vientos
MIC	22 49.55	70 13.96	1527	Michilla
ANG	23 06.04	70 30.70	710	Angamos
VAL	23 09.94	69 59.79	1400	Valenzuela
MAR	23 15.68	69 31.12	1720	Morrito
SCR	23 26.77	69 35.24	1820	San Cristobal
LMO	23 33.94	70 16.57	1000	Los Morros
AVI	24 06.73	69 15.38	2250	Augusta Victoria
CRI	24 10.03	70 22.27	1620	Cerro Sta. Rita

three-component L-2 (2 Hz) seismometers. The digital signals were multiplexed and registered on magnetic tapes. The time signals were obtained from the world-wide OMEGA system. (3) A telemetric digital network of seven stations with vertical L-4C (1 Hz) seismometers whose signals were radiotransmitted and recorded at a central station which was also equipped with a three-component L-22 (2 Hz) seismometer. The signals and the OMEGA time were multiplexed and recorded on magnetic tapes.

Location of the events

For the analogue records the accuracy of the P and S readings are estimated to be about 0.1 and 0.5 s, respectively, whereas for the digital stations the accuracy of these readings is about 0.01 and 0.2 s, respectively. The highest precision S-wave arrival times were obtained using the horizontal components of the digital instruments. For some periods the OMEGA clock was not synchronized with the radio signal at some GEOSTRAS stations. In these instances the absolute time was not available and only the polarity and the $S-P$ times were used.

Table 2. Velocity structure model used to locate hypocentres of the recorded events (modified from Wigger 1988).

Vp(km/s)	h(km)
5.5	00
6.2	06
6.8	10
7.2	29
8.0	55

The events were located using the HYPO71PC program (Lee & Valdes 1978). The velocity model used (Table 2) was inferred from the seismic refraction studies conducted by Wigger (1988) near Antofagasta. The readings with high residuals were verified and re-read.

The following parameters were varied to check the reliability of the solutions: (1) the initial depth, from 0 to 250 km in variable (10–25 km) intervals; (2) the velocity model was changed to a simple model consisting of a layer over a half-space; and (3) the V_P/V_S ratio was varied from 1.6 to 1.8 at 0.4 increments. An event location was considered reliable if it fulfilled the following criteria: (1) it had a minimum of 10 phase readings, including at least three S phases, and the distance between the epicentre and the nearest station with an S reading was smaller than the calculated depth; (2) the epicentral and depth variations were smaller than ±2.5 km when the initial depth and the velocity model were varied as described earlier; and (3) the epicentral and depth variations were less than ±5 km when the V_P/V_S ratio was varied from 1.6 to 1.8 at 0.4 increments.

With these criteria, 197 reliable locations were determined with magnitudes $2 \leqslant M_d \leqslant 5$ and RMS $\leqslant 0.3$ s. These events were then used as master events to relocate all the microearthquakes that did not fit the distance–depth criterion, but had at least 20 phase readings. Forty-eight events were thus relocated. The epicentral distribution of the reliable and relocated events is shown in Fig. 1. The magnitude M_d was estimated with the coda duration T and the epicentral distance D according to the relation given by Lee, Bennett & Meagher (1972), $M_d = 0.87 + 2\log(T) + 0.0035D$, where T is in seconds and D in kilometres.

No event was located from the trench to 80 km eastward with the criteria just described, probably due to the lack of off-coast coverage. The seismic activity is not evenly distributed but clusters in elongated bands nearly parallel to the coast and in intense swarms, particularly to the east. An important part of the seismicity took place eastward, outside the network.

Considering that the definition of the auxiliary nodal plane of the focal mechanisms is not always well constrained, a joint focal mechanism and stress tensor inversion was carried out from the first-motion polarities using the Rivera & Cisternas (1990) algorithm. The 15 individual and four composite focal mechanisms obtained are presented in Figs 2 and 3 (Table 3). The composite mechanisms (2, 5, 6 and 16; Table 3) combine events with epicentral and depth differences less than 10 km.

Six cross-sections from 0 to 600 km from the trench in the direction of the convergence of the Nazca plate with a width of 0.4°, were drawn using both reliable and relocated events (Figs 1 and 4). As the relocated events are mostly on the edges or outside the network, these events were included in the cross-sections mainly to obtain a more complete coverage of the coastal and down-dip parts of the slab. Lateral lower hemispheric projection of the focal mechanisms obtained are shown in Fig. 5.

RESULTS

Wadati–Benioff zone

We found that at shallow depths (20–70 km) the dip angle of the subducting plate is about 18° and at greater depths (70–250 km) the dip angle steepens to about 30° (Fig. 5). These values agree with those determined using global data (Jarrard 1986).

The cross-sections C2, C3 and C4 show a weak activity within the area of the network coverage, at distances between 150 and 220 km from the trench (Fig. 4). This decrease in seismic activity is not observed in C1 and C5. The C6 cross-section corresponds to the southern edge of the network, and it will not be included in the following discussion because it has only a few events, and most of these are relocated microearthquakes. A similar pattern of seismic activity is also observed in other parts of the subduction zone along South America, for example, in southern Peru (Grange *et al.* 1984).

Another absence of seismicity is observed from about 130 to 200 km depth along the slab. This absence is well correlated with the presence of the active volcanoes in the Andean range and it probably corresponds to partial melting of the upper part of the subducted slab.

In the C3, C4, C5 and C6 cross-sections, a cluster of seismicity is also observed at depths between 200 and 260 km.

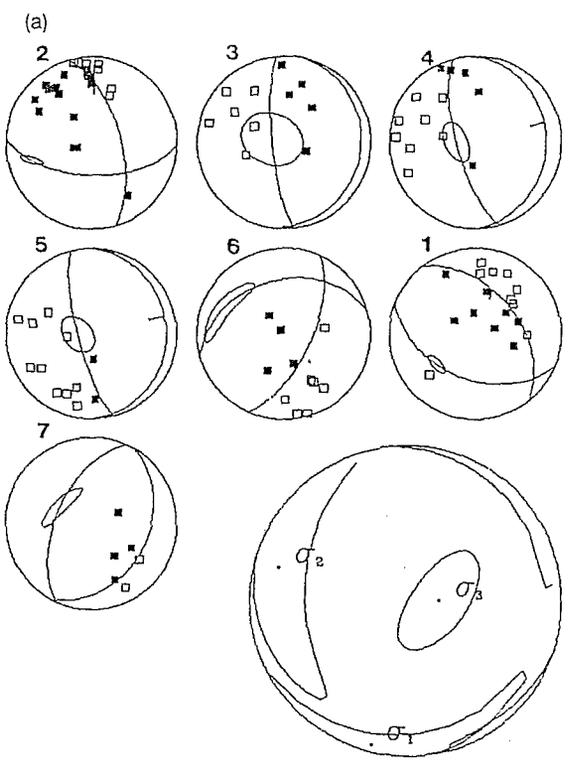

Figure 2. (a) Joint focal mechanism and stress tensor inversion solutions from the first-motion polarities using the Rivera & Cisternas (1990) algorithm for the reverse faulting events. Open squares denote dilation and closed squares denote compression. An estimation of the uncertainty of the fault-plane pole is shown for each mechanism. In the lower part of the figure the orientation and the associated uncertainty of the compressional (σ_1), tensional (σ_3), and intermediate (σ_2) axis of the obtained stress tensor are also presented. (b) Joint focal mechanisms and stress tensor inversion solutions from the first-motion polarities using the Rivera & Cisternas (1990) algorithm for the normal faulting events. Symbols as in Fig. 2(a). When there is no uncertainty region for the fault-plane pole, it means that the fault planes are not well constrained.

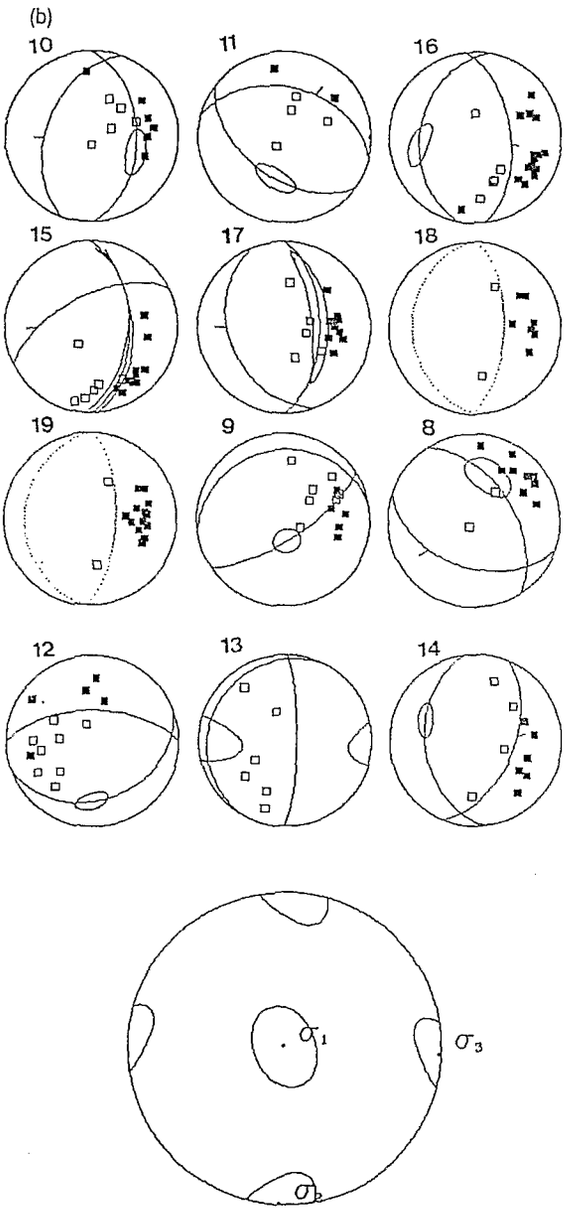

Figure 2. (*Continued.*)

Table 3. Focal mechanism solutions obtained from the first-motion polarities using the Rivera & Cisternas (1990) algorithm. No = identification number of the event, same used in Figs 2, 3 and 5; $\phi°$, $\delta°$, $\lambda°$ = strike, dip and rake of the focal mechanism; H = depth in kilometres; and M_d coda-duration magnitude according to the relation given by Lee *et al.* (1972).

N°	FAULT PLANE			DEPTH	MAGNITUDE
	$\phi°$	$\delta°$	$\lambda°$	H	Md
1	321.8	48.1	111.0	52	3.2
2*	344.0	62.6	144.3	40-48	3.2-3.4
3	11.9	12.5	107.2	34	2.8
4	359.2	18.9	104.2	32	2.4
5*	359.7	13.5	103.7	41-47	2.7-2.7
6*	24.3	64.5	62.7	56-63	2.9-2.9
7	28.9	34.1	93.9	69	2.8
8	108.4	45.1	-119.5	80	4.2
9	260.5	20.0	-67.0	99	3.5
10	200.4	45.7	-74.7	85	3.4
11	283.7	41.8	-106.9	78	2.9
12	270.2	60.2	-79.7	52	3.1
13	0.8	79.6	-95.7	38	2.2
14	22.4	53.0	-71.6	68	3.1
15	243.4	60.6	-44.2	81	3.8
16*	353.3	55.7	-99.5	81-74	3.6-3.7
17	158.3	35.3	-107.8	104	3.6
18	180.8	24.7	-91.3	106	3.5
19	177.1	28.2	-94.0	117	3.6

Reverse faulting events

Three shallow-dipping thrust faulting focal mechanism solutions were determined; two for individual earthquakes (3 and 4) and the third a composite solution of two events (5) (Fig. 3a, Table 3). Within the uncertainties of the poorly constrained nodal plane of the focal mechanism solutions of these thrust events (indicated in Fig. 2), we can conclude that the average slip direction of these events is not in contradiction with that estimated in the region from global plate tectonic models (N77°E, NUVEL 1; DeMets *et al.* 1990).

The depth of the thrust events varies from 32 to 47 km at distances between 90 and 140 km from the trench (Fig. 5). The seismogenic interplate contact thus reaches at least 47 km depth. This depth is about twice the maximum depth observed for Guerrero, Mexico (20–25 km) and it is in accordance with the scale relation 2:1 pointed out by Suárez *et al.* (1990) for the subduction zones of Mexico and Chile.

Four reverse faulting mechanisms with a high dip angle were also determined (1, 2, 6 and 7; Fig. 3a). These events occurred from 120 to 200 km from the trench at depths varying from 40 to 78 km and should be interpreted as a result of faulting within the subducted slab (Fig. 5).

Shallow normal faulting events

Two normal faulting focal mechanisms were determined (12 and 13; Fig. 3b; Table 3). The events occurred at a distance of 130 km from the trench at depths of 38 and 52 km, respectively, in the same distance range from the trench where thrust faulting is also observed (Fig. 5). The tensional field associated with these events contrasts with the compressional field found at the same distances from the trench and at about the same depths. These epicentres are close to the site where the main branch of the Atacama fault changes its azimuth from N45°E to a more north–south direction (Fig. 3b). Considering the depth of both events it is difficult to associate them with the Atacama fault system, and in Fig. 5 it can be observed that they are clearly inside the Wadati–Benioff plane. More data are needed to establish if there is a relation between the two phenomena.

Intermediate depth normal faulting events

10 normal faulting events were determined (8, 9, 10, 11, 14, 15, 16, 17, 18 and 19; Fig. 3b; Table 3). These intraplate events occurred at distances of above 200–290 km from the trench and their depths varied from 68 to 85 km (Fig. 5). Therefore, a change from a compressional to a tensional stress field can be observed at approximately 200 km from the trench, corresponding to a depth of about 70 km.

Crustal seismicity

12 microearthquakes were located with depths shallower than 30 km (Fig. 6). However, most of them have epicentres in the ocean and are probably associated with the slab. One event close to the main branch of the Atacama fault system had a depth of 28 km, its focal mechanism is not reliable, and it is probably associated with the subduction of the Nazca plate and does not reflect crustal deformation of the overlying plate (Fig. 5).

A cluster of three events (shown by crosses in Fig. 6) with depths less than 5 km corresponds to blasts in the Mantos Blancos mine. Thus we conclude that no shallow microearthquake associated with the Atacama fault system occurred during the period of the experiment.

DISCUSSION

Seismogenic plate contact

The seismogenic coupled zone corresponds to the interplate contact that can generate large underthrusting events. The maximum depth of the coupled–uncoupled transition has been determined using the observed maximum depth of the shallow-dipping thrusting fault event using teleseismic data (e.g. Tichelaar & Ruff 1991; Pacheco, Sykes & Scholz 1993).

Local microseismic experiments offer the possibility of estimating the maximum depth of the coupled interplate region. The expected behaviour of the stress acting along the slab is a compressional field in the contact zone and a tensional field from the coupled–uncoupled transition. This possibility is particularly useful for subduction regions that have local networks with inadequate azimuthal coverage for thrust events which occur mainly offshore, and which have generally unreliable data on the location and focal mechanisms of earthquakes. In these regions the transition occurs inland and within the coverage of local networks. Therefore, the depth of the change between the compressional and tensional stress field along the slab could be an advantageous alternative method to estimate the maximum depth of the coupled zone.

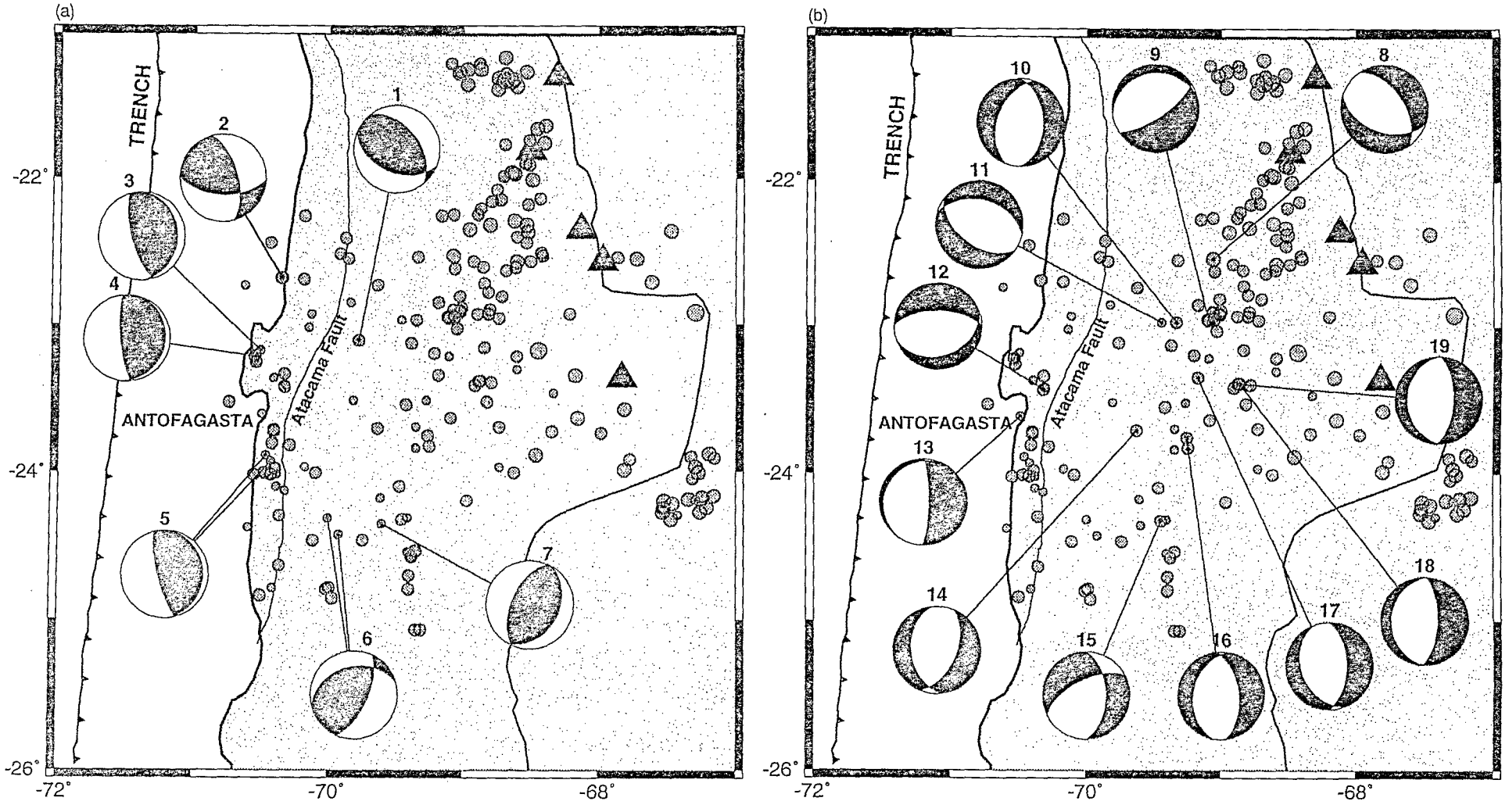

Figure 3. (a) Focal mechanism solutions in lower hemispheric projection of shallow-dipping and high-angle reverse faulting events. The epicentral distribution of the reliable seismicity recorded during the experiment is also presented. The number in the upper part of each mechanism corresponds to its identification number (Fig. 5, Table 3). Symbols as in Fig. 1. (b) Focal mechanism solutions in lower hemispheric projection of normal faulting events. Symbols as in Fig. 3(a).

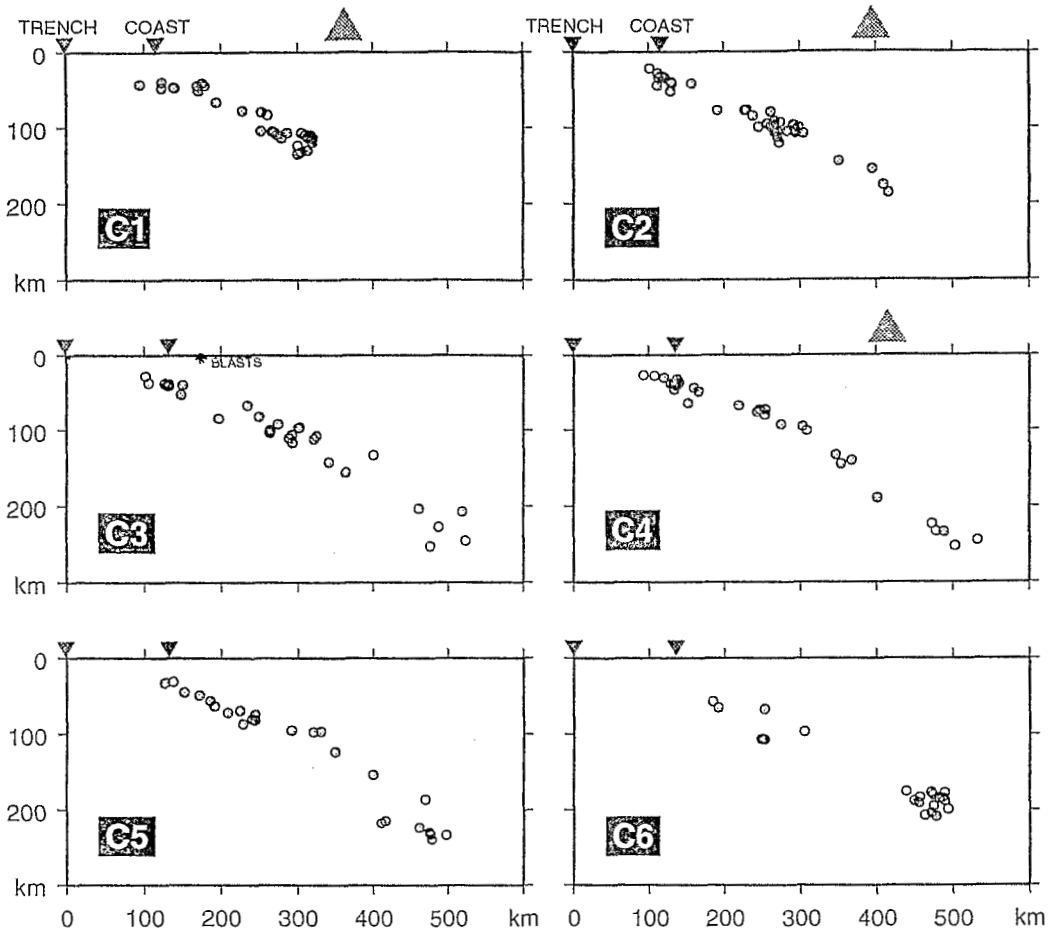

Figure 4. Depth distribution in the direction of the Nazca plate convergence direction of the reliable (dotted circles) and relocated (open circles) events of the six cross-sections indicated in Fig. 1. The projection of the trench, the coastline and the volcano (shaded triangles) are also shown. Crosses in C3 profile correspond to the Mantos Blancos mineblast.

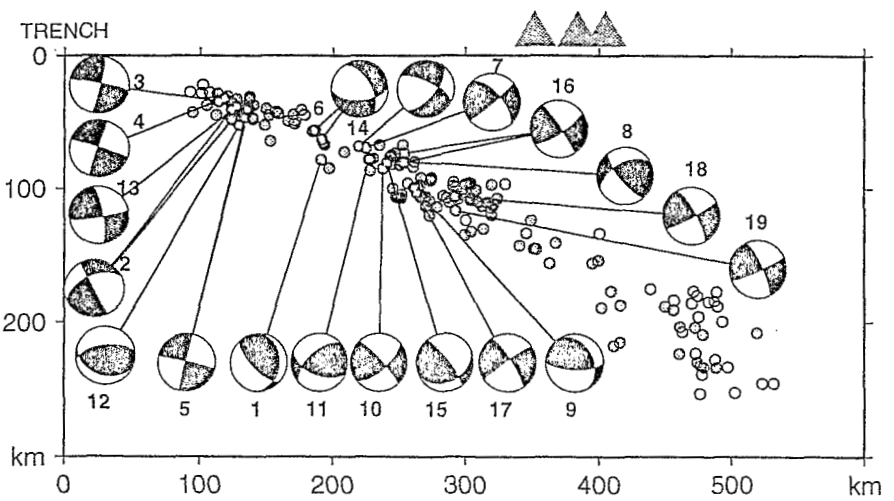

Figure 5. Composite depth distribution from C1 to C6 cross-section from Fig. 4. The lateral lower hemispheric focal mechanism solutions obtained are also shown. Each mechanism is identified by its number and is keyed to Table 3.

In the Antofagasta field experiment we observed that the maximum depth of the shallow-dipping thrusting faulting events is about 47 km, the high-angle reverse faulting events occur in the range 40–78 km depth, and the deeper normal faulting events occur between 68 and 85 km depth (Fig. 5). Therefore a change from a compressional to a tensional stress field along the slab occurs about 70 km depth and at distances of around 200 km from the trench; this corresponds approximately to the Precordillera. The depth of the change in stress along the slab correlates with the crustal thickness of about 70 km under the Precordillera determined by refraction and gravity studies (Wigger 1988). We cannot distinguish whether the high-dipping reverse faulting events are on the interplate contact or below it, but we can follow the change in compressional to tensional stress field along the slab.

The minimum depth of the seismogenic zone could be considered to be about 10–15 km; at shallower depths the poorly consolidated sediments that form the accretionary prism can deform aseismically (Byrne, Davis & Sykes 1988; Marone & Scholz 1988).

There are therefore two possibilities: (1) the coupled zone extends from 10–15 to 47 km in depth, with a seismogenic contact zone width of about 90 km; and (2) the coupled zone extends to about 70 km depth, where the transition from the compressional to tensional stress field is observed. In this instance the width of the seismogenic coupled zone could reach about 130 km.

If we assume the rupture length of 420 km determined by Comte & Pardo (1992) for the 1877 earthquake and considering the two seismogenic contact widths determined earlier, the maximum magnitude M_S (Kanamori & Anderson 1975) estimated for the zone varies between 8.6 and 8.7.

Crustal seismicity

In a preliminary report Comte *et al.* (1992) associated some shallow events with the Atacama fault system. However, when the digital data were included in the analysis, these events were relocated within the subducted slab; therefore, during this seismic experiment, no shallow event could be associated with the Atacama fault system.

Armijo & Thiele (1990) proposed a ramp model to explain the left-lateral displacements observed in the central part of the Atacama fault system, instead of the right-lateral displacements which should be expected from the orientation of the fault and the direction of the Nazca plate convergence. This model assumes that the Coastal Scarp and the Atacama fault may interact with the subduction interface at depth, with two changes in the dip angle of the descending slab: one located at approximately 25 km depth and at a distance of about 80 km from the trench associated with the Coastal Scarp; and the second change located at approximately 50 km depth, at a distance of 150 km from the trench. Armijo & Thiele (1990) argue that this change in dip controls the geometry of the Atacama fault system. The first change that occurs under the ocean cannot be verified with the data collected during this experiment because the coverage of the network was mainly inland; the second change does occur within the network coverage and it is not observed on the various cross-sections, where the slab appears as a smooth surface.

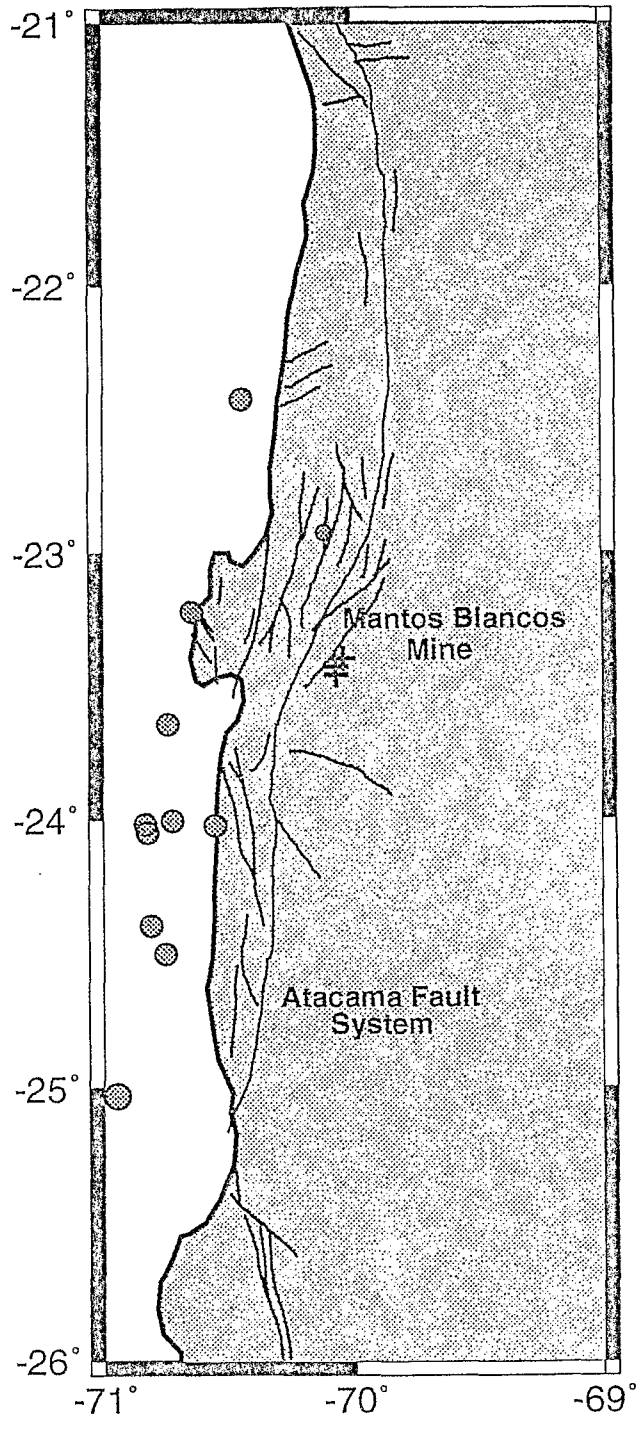

Figure 6. Shallow seismicity near the Atacama fault system. *Crosses indicate the three explosions in the Mantos Blancos mine* which occurred during this experiment.

Based on seismic experiments of short duration it is not always possible to define whether a continental fault system is active. It has been observed that the most active segments of a fault, from a microseismic point of view, are not necessarily the same segments that can generate major earthquakes (Wesnousky 1990). Thus the lack of shallow

seismic activity associated with the Atacama fault system during the September and October 1988 field experiment does not constitute a strong argument in favour of the hypothesis of Yañez (in preparation), who considers that this fault is no longer active.

CONCLUSIONS

An alternative method is suggested to estimate the depth of the coupled–uncoupled transition in the subduction lithosphere using reliable local data, defined by the depth where a change from compressional to tensional stress field along the slab is observed.

In the case of Antofagasta, northern Chile, two estimates of the maximum depth of the seismogenic coupled zone are obtained, one defined by the maximum depth of the shallow-dipping thrust events and the other defined by the depth where the change from a compressional to a tensional stress field is observed. In the first instance we obtain a maximum depth of 47 km with a width of the seismogenic contact zone of about 90 km. In the second we obtain a maximum depth of 70 km, with a corresponding width of the seismogenic contact zone of about 130 km. With the two width estimations of the seismogenic zone, the maximum magnitude, M_S expected for the studied region could reach about 8.6–8.7.

No shallow event associated with the Atacama fault system was observed during the experiment. The ramp and lateral decoupling along the subduction plate boundary model proposed by Armijo & Thiele (1990) for the central part of this fault system is not confirmed by the geometry of the Wadati–Benioff zone determined in this study.

ACKNOWLEDGMENTS

We sincerely thank G. Suárez, S. K. Singh, and D. Byrne for their helpful comments. This work has greatly benefited from critical reviews by P. Bernard and H. Lyon-Caen. This research was partially supported by ORSTOM and the Fundación Andes-Chile, grant C-52040. We also thank the Chilean and French staff for their participation during the field work.

REFERENCES

Arabasz, W. J., 1971. Geological and geophysical studies of the Atacama fault zone in northern Chile, *PhD thesis*, California Institute Technology, Pasadena.

Araujo, M., 1985. Estudio de sismos en el noreste argentino mb > 5.6 mediante mechanismos de foco y modelado de ondas de cuerpo, *MSc thesis*, Facultat de Ciencias-UNAM, Mexico.

Armijo, R. & Thiele, R., 1990. Active faulting in northern Chile: ramp stacking and lateral decoupling along a subduction plate boundary? *Earth planet. Sci. Lett.*, **98**, 40–61.

Barazangi, M. & Isacks, B., 1976. Spatial distribution of earthquakes and subduction of the Nazca plate beneath South America, *Geology*, **4**, 686–692.

Byrne, D., Davis, D. & Sykes, L., 1988. Loci and maximum size of thrust earthquakes and the mechanics of the shallow region of subduction zones, *Tectonics*, **7**, 833–857.

Chowdhury, D. K. & Whiteman, S. K., 1987. Structure of the Benioff zone under southern Peru to central Chile, *Tectonophysics*, **134**, 215–226.

Comte, D. & Pardo, M., 1991. Reappraisal of great historical earthquakes in the Northern Chile and Southern Peru sesmic gaps, *Natural Hazards*, **4**, 23–44.

Comte, D., Pardo, M., Dorbath, L., Dorbath, C. Haessler, H., Rivera, L., Cisternas, A. & Ponce, L., 1992. Crustal seismicity and subduction morphology around Antofagasta, Chile: preliminary results from a microearthquake survey, *Tectonophysics*, **205**, 13–22.

DeMets, C., Gordon, R. G., Argus, D. F. & Stein, S., 1990. Current plate motions, *Geophys. J. Int.*, **101**, 425–478.

Dorbath, L., Cisternas, A. & Dorbath, C., 1990. Quantitative assessment of great earthquakes in Peru, *Bull. seism. Soc. Am.* **80**, 551–576.

Grange, T., Hatzfield, D., Molnar, P. Roecker, S., Suarez, G., Rodriguez, A. & Ocola, L., 1984. Microearthquake activity and fault plane solutions in southern Peru and their tectonic implications, *J. geophys. Res.*, **89**, 6139–6152.

Isacks, B., 1988. Uplift of the central Andean plateau and bending of the Bolivian orocline, *J. geophys. Res.*, **93**, 3211–3231.

Jarrad, R., 1986. Relations among subduction parameters, *Rev. Geophys.*, **24**, 217–284.

Kanamori, H. & Anderson, D., 1975. Theoretical basis of some empirical relations in seismology, *Bull. seism. Soc. Am.*, **65**, 1073–1095.

Kelleher, J., 1972. Rupture zones of large South American earthquakes and some predictions, *J. geophys. Res.*, **77**, 2087–2103.

Lee, W. & Valdes, C. M., 1978. HYPO1PC: a personal computer version of the HYPO71 earthquake location program, *US Geological Survey, Open File Report* 85-749.

Lee, W., Bennett, R. & Meagher, K., 1972. A method of estimating magnitude of local earthquakes from signal duration, *US Geological Survey, Open File Report* 28.

Marone, C. & Scholz, C., 1988. The depth of seismic faulting and the upper transition from stable to unstable slip regimes, *Geophys. Res. Lett.*, **15**, 621–624.

McCann, W., Nishenko, S. P., Sykes, L. R. & Krause, J., 1979. Seismic gaps and plate tectonics: seismic potential for major boundaries, *Pure appl. Geophys.*, **117**, 1082–1147.

Naranjo, J. A., 1987. Interpretación de la actividad cenozoica superior a lo largo de la zona de la falla de Atacama, Norte de Chile, *Rev. Geol. Chile*, **31**, 43–55.

Nishenko, S., 1985. Seismic potential for large and great interplate earthquakes along the Chilean and southern Peruvian margins of South America: a quantitative reappraisal, *J. geophys. Res.*, **90**, 3589–3615.

Pacheco, J. F., Sykes, L. R. & Scholz, C., 1993. Nature of seismic coupling along simple plate boundaries of the subduction type, *J. geophys. Res.*, **98**, 14133–14160.

Rivera, L. & Cisternas, A., 1990. Stress tensor and fault plan solutions for a population of earthquakes. *Bull. seism. Soc. Am.*, **80**, 600–614.

Suárez, G., Monfret, T., Wittlinger, G. & David, C., 1990. Geometry of subduction and depth of the seismogenic zone in the Guerrero gap, Mexico, *Nature*, **345**, 336–338.

Tichelaar, B. & Ruff, L., 1991. Seismic coupling along the Chilean subduction zone, *J. geophys. Res.*, **96**, 11 997–12 022.

Wesnousky, S. G., 1990. Seismicity as function of cumulative geologic offset: some observations from southern California, *Bull. seism. Soc. Am.*, **80**, 1374–1381.

Wigger, P. J., 1988. Seismicity and crustal structure of the central Andes, in: *The Southern Central Andes. Contributions to Structure and Evolution of an Active Continental Margin, Lecture Notes in the Earth Sciences*, pp. 209–227, eds Reuter, Scheuber & Wigger, Springer, Berlin.